QIRT'2022

10.21611/qirt.2022.2023

16th Quantitative InfraRed Thermography Conference

Impact of Temperature on Resonant Tank Components in LLC Resonant SMPS

by R. Kasikowski *, B. Więcek *

* Łódź Univ. of Technology, 90-924, Wólczańska Str, Łódź, Poland, rafalkasikowski@dokt.p.lodz.pl

Abstract

LLC resonant topology contains a resonant tank consisting essentially of three components, namely the primary inductance of a transformer, a resonant inductance and a resonant capacitor. The operating frequency of the LLC converter is finely tuned to match the resonant frequency of the resonant inductance and capacitor, at which point electric current through the tank is, effectively, sinusoidal. The parameters of the resonant tank are temperature dependent and therefore changes in the capacitance and inductance of the resonant components, and, by extension, in the resonant frequency, occur. This results in the distortion of the current, and the efficiency of power conversion is affected. Herein, IR thermography is utilized to determine the steady-state operating temperature of LLC resonant tank components and hence the impact of temperature on the resonant frequency and operation of LLC SMPSs (switch-mode power supplies) can be ascertained.

1. Introduction

The stability of the resonant capacitor dielectric, the transformer magnetic core permeability and the resonant inductance, in relation to temperature, is critical, as all impact the operating frequency of the LLC converter. A typical LLC resonant converter consists of three sections [1]: a switch network, an LLC resonant tank and a rectifier network, as shown in Figure 1.

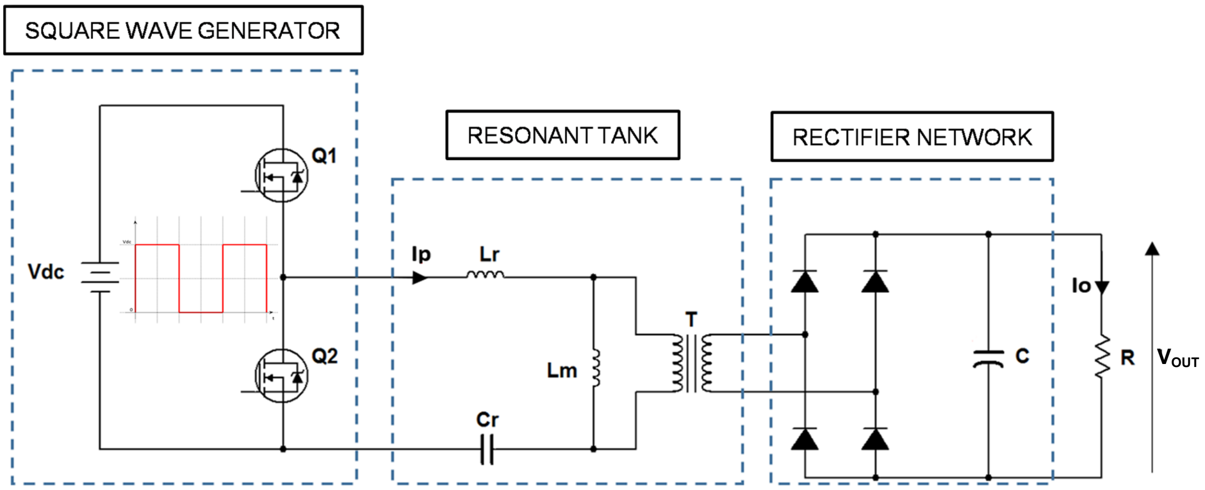

Fig. 1. *Schematic of half-bridge LLC resonant converter.*

The resonant tank essentially responds only to fundamental components of the applied waveforms and effectively filters higher harmonics, the schematic in Figure 1 can be, for all intents and purposes, represented by applying fundamental harmonic approximation (FHA), with the AC equivalent circuit of Figure 2 which assumes that only the fundamental harmonic V_{ac} of the driving voltage V_{dc} contributes to power transfer to the output [2]. The reflected output voltage and the equivalent load resistance are denoted by $n \cdot V_s'$ and R_{ac}, respectively, where n stands for the turn ratio of the transformer.

The circuit in Figure 2 can be used to derive the gain characteristics (see Figure 3) of the LLC resonant converter in the form of a transfer function (Eq. 1) representing the relationship between the input and output voltage for a full spectrum of frequencies ($s = j \cdot \omega$).

$$H(s) = \frac{n \cdot V_s'(s)}{V_{ac}(s)} = \frac{R_{ac} \| sL_m}{\frac{1}{sC_r} + sL_r + R_{ac} \| sL_m} = \frac{\frac{s^2}{\omega_0^2}(m-1)}{\left(\frac{s^2}{\omega_P^2}+1\right) + \frac{s}{\omega_0}\left(\frac{s^2}{\omega_0^2}+1\right)(m-1)Q} \quad (1)$$

where:
ω_0 is the resonant frequency determined by L_r and C_r
ω_p is the resonant frequency determined by $(L_m + L_r)$ and C_r
m is the ratio $(L_m + L_r)/ L_r$
$(L_m + L_r) = L_p$ is the inductance determining resonant frequency ω_p
Q is given by $\sqrt{\frac{L_r}{C_r} \cdot \frac{1}{R_{ac}}}$ and represents output loading

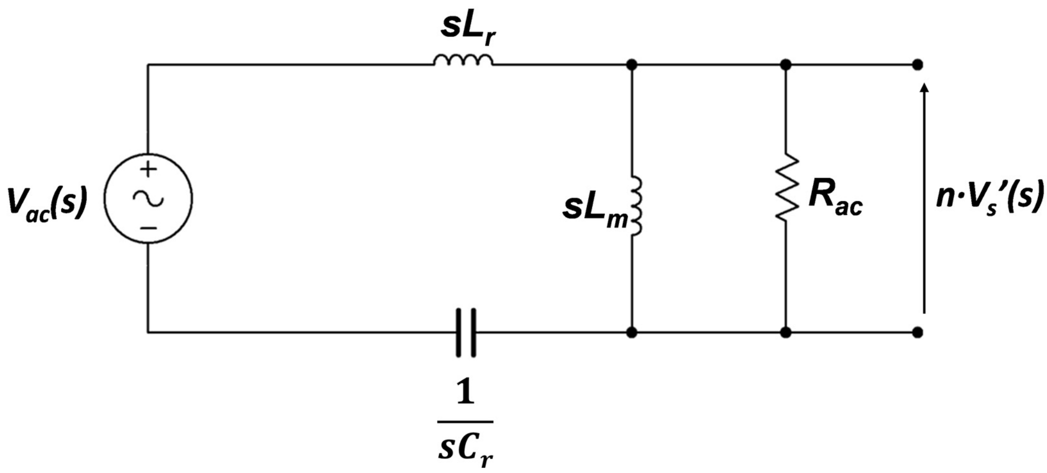

Fig. 2. *AC equivalent circuit for LLC resonant converter.*

The absolute value of transfer function *H(s)* is defined as a magnitude or voltage gain *G* (Eq. 2) which constitutes the gain characteristics of LLC type converters. These are shown below for selected values of *Q* factor representing various output loading conditions.

$$G = |H(s)| = \left| \frac{\frac{\omega^2}{\omega_0^2}(m-1)}{\left(\frac{\omega^2}{\omega_P^2} - 1\right) + j\frac{\omega}{\omega_0}\left(\frac{\omega^2}{\omega_0^2} - 1\right)(m-1)Q} \right| \tag{2}$$

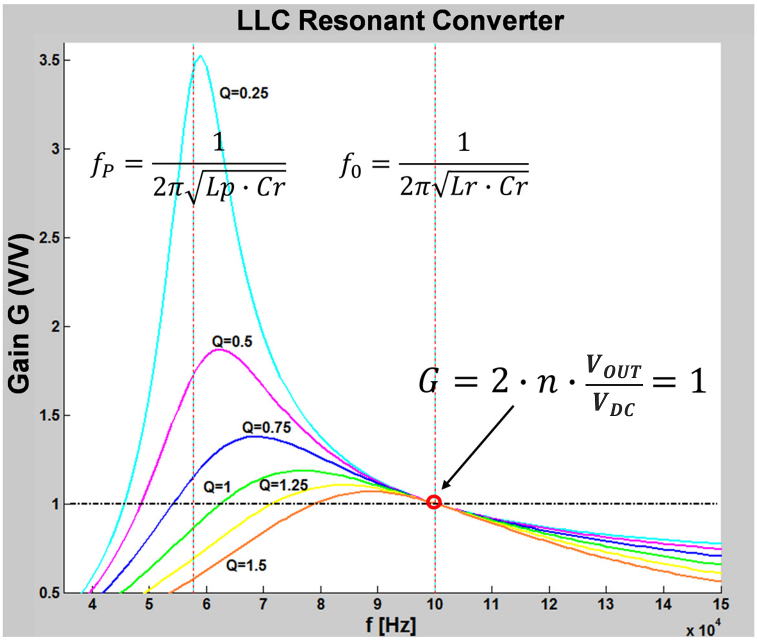

Fig. 3. *Typical gain characteristics of LLC resonant converter.*

Magnetic components, be they inductors or transformers, are some of the bulkiest and least cost-effective elements of any SMPS. What is more, they constitute a considerable source of power dissipation. The resonant LLC solution gives an opportunity to remove one of the resonant tank components, the resonance inductance, and utilize leakage inductance of the transformer in its place. The integrated LLC transformer approach requires a noticeably distinctive design of the component, as primary and secondary sides display an impaired magnetic coupling that results in the leakage/resonant inductance design engineers are aiming for. The leakage inductance exists not only in the primary side, but also in the secondary side, and this significantly alters the equivalent circuit for the LLC resonant converter in Figure 1 and Figure 2 [3]. The resulting circuit accommodates the secondary-side leakage inductance as shown in Figure 4.

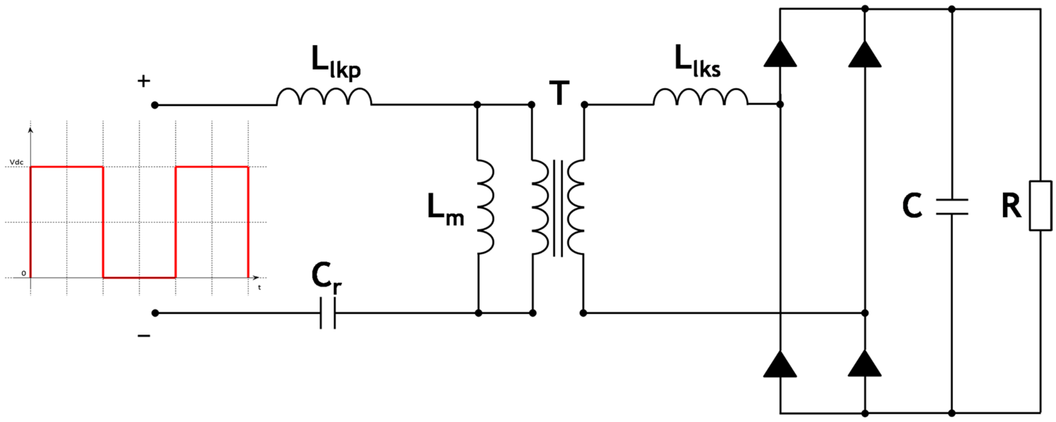

Fig. 4. *Modified circuit showing secondary-side leakage inductance of LLC resonant converter.*

The voltage gain *G* derived from Figure 4 for the LLC resonant converter with an integrated transformer is as follows (Eq. 3):

$$G = |H(s)| = \left| \frac{\frac{\omega^2}{\omega_0^2}\sqrt{m(m-1)}}{\left(\frac{\omega^2}{\omega_P^2} - 1\right) + j\frac{\omega}{\omega_0}\left(\frac{\omega^2}{\omega_0^2} - 1\right)(m-1)Q} \right| \tag{3}$$

As one can notice in Figure 5, the implementation of the integrated LLC transformer approach yields a somewhat larger gain for resonant frequency f_0 than that observed for a conventional LLC resonant circuit with a separate resonant inductor.

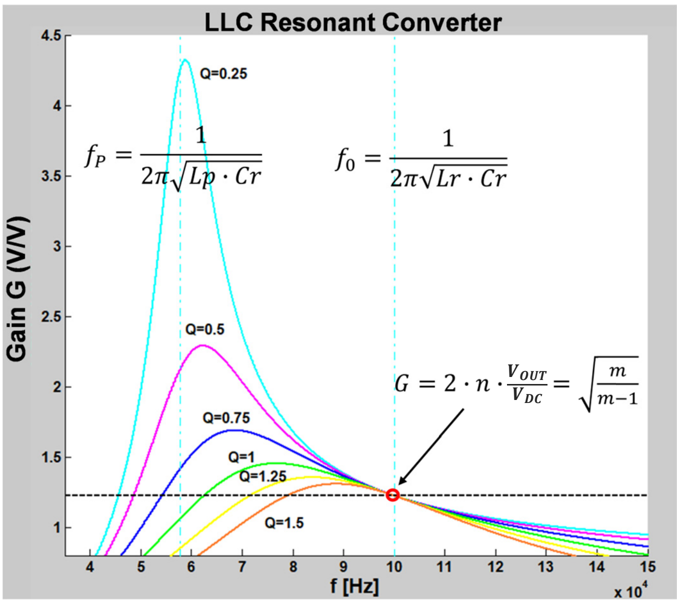

Fig. 5. *Typical gain characteristics of LLC resonant converter with integrated transformer.*

As stated herein, the physical properties of LLC resonant tank components are temperature-dependent, and as a result the evolution of the resonant parameters with operating temperature will have an observable impact on the gain characteristics as well as the shape of the current through the resonant tank which may somewhat deviate from the desirable sinusoidal shape (Figure 6) [4].

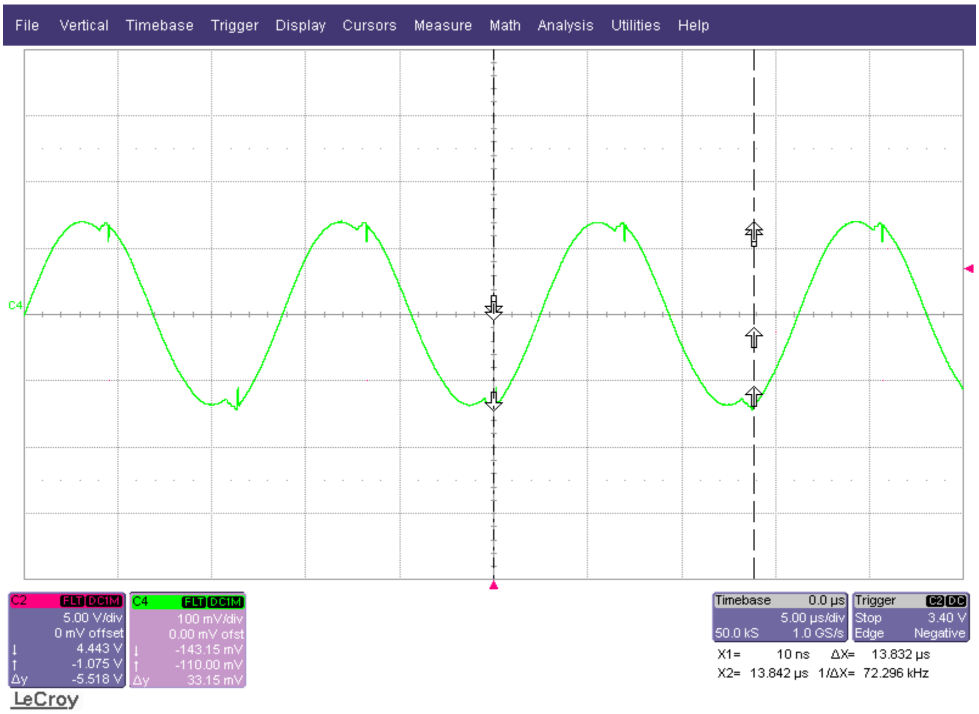

Fig. 6. *Typical resonant tank current waveform.*

2. Investigated LLC resonant converter

The analysis of the variations of the LLC resonant network parameters with temperature was carried out for the constructed LLC converter shown in Figure 7. The implemented LLC solution is of the integrated type hence the resonant circuit consists of two physical components, the LLC transformer and the resonant capacitor, whereas the leakage inductance of the transformer is utilized as the resonant inductance. The individual design parameters of the constructed LLC resonant tank are listed in Table 1.

Table 1. *LLC resonant network design parameters.*

LLC converter parameters	**Symbol**	**Value**
Input voltage	V_{DC}	400 VDC
Output voltage	V_{OUT}	24 VDC
Power	P_{OUT}	180 W
Resonant capacitance	C_r	33 nF
Resonant inductance	L_r	120 µH
Resonant frequency	f_0	80 kHz
Primary inductance	L_P	600 µH
L_P/L_r ratio	m	5
Resonant frequency for L_P	f_p	36 kHz

As indicated in Table 1, the resonant frequency of the circuit is about 80 kHz and, if constructed properly, the LLC converter should, for given input and output parameters, operate at the said frequency for any loading conditions. This independence of the operating frequency from loading conditions at the resonant point is one of the key features of LLC topology. Placing switching frequency at or in the immediate vicinity of the resonant frequency f_0 for the resonant capacitor C_r and the resonant inductance L_r ensures that the LLC converter exhibits so-called soft switching [5], and current waveforms through the resonant tank closely resemble purely sinusoidal shapes.

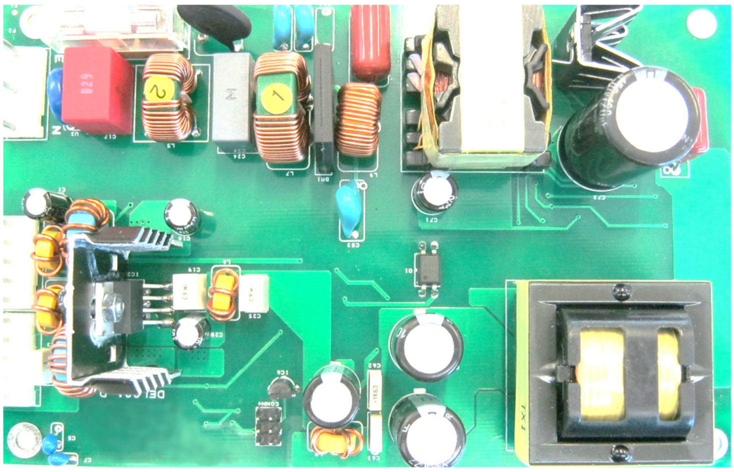

Fig. 7. *Constructed LLC SMPS.*

3. Impact of temperature on parameters of resonant tank

The ascertainment of the evolution of the resonant parameters with operating temperature was carried out in a thermal test chamber (Figure 8) for the components as listed in Table 2.

Table 2. *Investigated LLC resonant network components.*

Component	Symbol	Construction
Resonant capacitor 1	C_{r1}	Film, Double Metallized PP
Resonant capacitor 2	C_{r2}	Film, Double Metallized PP
Resonant capacitor 3	C_{r3}	Film, Double Metallized PP
Resonant capacitor 4	C_{r4}	SMD MLCC, X7R
Resonant capacitor 5	C_{r5}	Film, Single Metallized PP
Resonant capacitor 6	C_{r6}	SMD MLCC, C0G/NP0
Resonant capacitor 7	C_{r7}	SMD MLCC, X8G
Primary inductance	L_P	3C95
Resonant inductance	L_r	Leakage Inductance

Capacitors selected for resonant applications, or the configuration in which they are combined, have to show a relatively high AC current capability. The components should also display high stability with voltage, temperature and humidity.

Fig. 8. *Thermal test chamber used in experiment.*

Initially, the parameters of the components in Table 2 were determined at an ambient temperature of about 25 ˚C. Subsequently, the internal ambient in the chamber was gradually increased with a step of 5 ˚C up to 105 ˚C as this was the lowest maximum operating temperature of all the tested components. The values of capacitance and inductance of the investigated component were determined with a PeakTech 2170 digital LCR/ESR meter at a frequency of 100 kHz so as to recreate the operating conditions of the resonant tank components as closely as possible. The value of capacitance and the value of inductance are both functions of operating frequency, and therefore it was deemed necessary to carry out the measurement at a frequency nearing the resonant frequency at which the converter operates. The results of the thermal measurements are shown in Figure 9 and Figure 10.

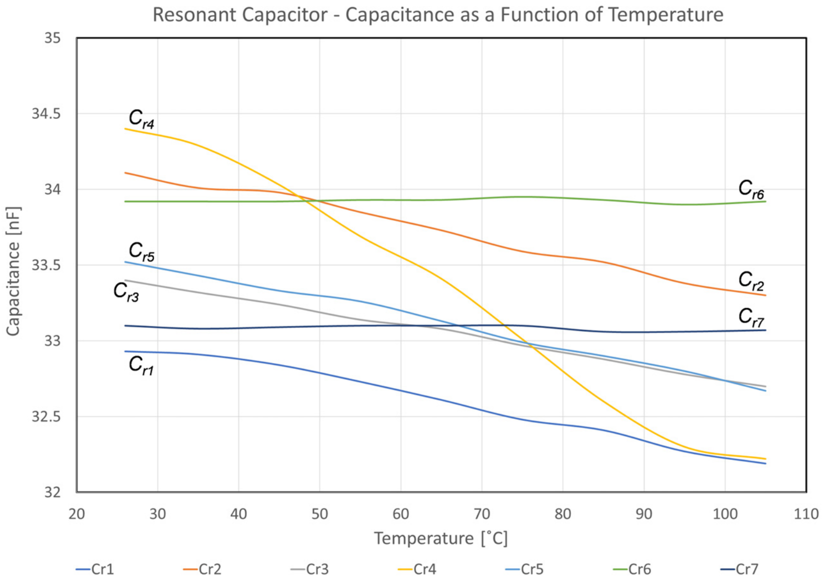

Fig. 9. *Results of thermal measurements for capacitors in Table 2.*

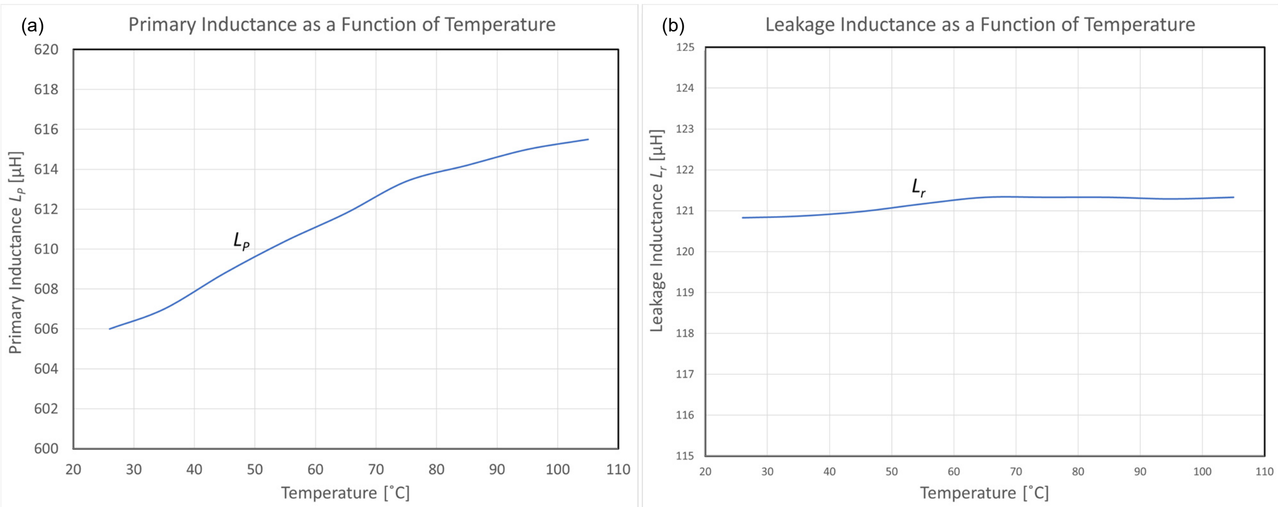

Fig. 10. *Results of thermal measurements for primary (a) and leakage inductance (b) in Table 2.*

Examining the outcomes of thermal measurements in the test chamber one can notice that capacitor C_{r6} and C_{r7} with C0G/NP0 and X8G dielectric respectively display the best thermal performance, and as such would be an ideal choice to feature in an LLC resonant tank under considerable thermal stress. As expected, C_{r4}, an X7R-dielectric capacitor, although typically considered as temperature-stable, showed inferior thermal performance in comparison with the rest of the capacitors in the set tested.

The primary inductance of the LLC transformer and the way it evolved with temperature appears to be in compliance with the manufacturer's datasheet for 3C95 ferrite core material [6], where the magnetic permeability of the material seems to be relatively temperature-stable with a minor increase for higher temperatures with respect to the ambient of 25 ˚C. The resonant or leakage inductance of the constructed LLC integrated transformer, as presumed, remained largely unaffected by rising temperature, with negligible fluctuations that could be attributed to a thermal expansion of the materials used in the construction of the transformer.

Assuming the worst-case operating conditions for the investigated resonant components and the implementation of the capacitor displaying the most inferior thermal performance, the initial parameters measured at the ambient of 25 ˚C would transform into those ascertained at 105 ˚C, as shown in the Table 3.

Table 3. *Parameters of investigated LLC resonant network components at 25 ˚C and 105 ˚C.*

Component	Symbol	Construction	Parameter @ 25 ˚C	Parameter @ 105 ˚C
Resonant capacitor	C_{r4}	SMD MLCC, X7R	34.4 nF	32.22 nF
Primary inductance	L_P	3C95	606 µH	615.5 µH
Resonant inductance	L_r	Leakage inductance	120.83 µH	121.33 µH

The figures from Table 3 can be used to calculate the resonant frequencies for the two scenarios and, by utilizing Eq. (3), the voltage gain characteristics for the LLC resonant converter at 25 ˚C as well as at 105 ˚C can be composed, as seen in Figure 11 and Figure 12, respectively.

$$f_{0(@25C)} = \frac{1}{2\pi\sqrt{L_r C_r}} = 78\ \mathrm{kHz}$$

$$f_{p(@25C)} = \frac{1}{2\pi\sqrt{L_p C_r}} = 34.8\ \mathrm{kHz}$$

$$m_{(@25C)} = \frac{L_p}{L_r} = 5.015$$

$$f_{0(@105C)} = \frac{1}{2\pi\sqrt{L_r C_r}} = 80.5\ \mathrm{kHz}$$

$$f_{p(@105C)} = \frac{1}{2\pi\sqrt{L_p C_r}} = 35.74\ \mathrm{kHz}$$

$$m_{(@105C)} = \frac{L_p}{L_r} = 5.073$$

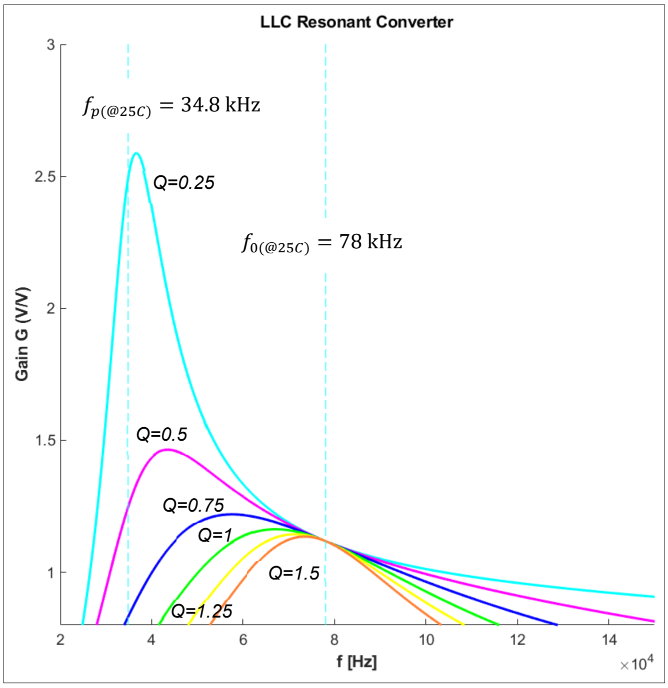

Fig. 11. *Gain characteristics of investigated LLC resonant converter at* 25 ˚C.

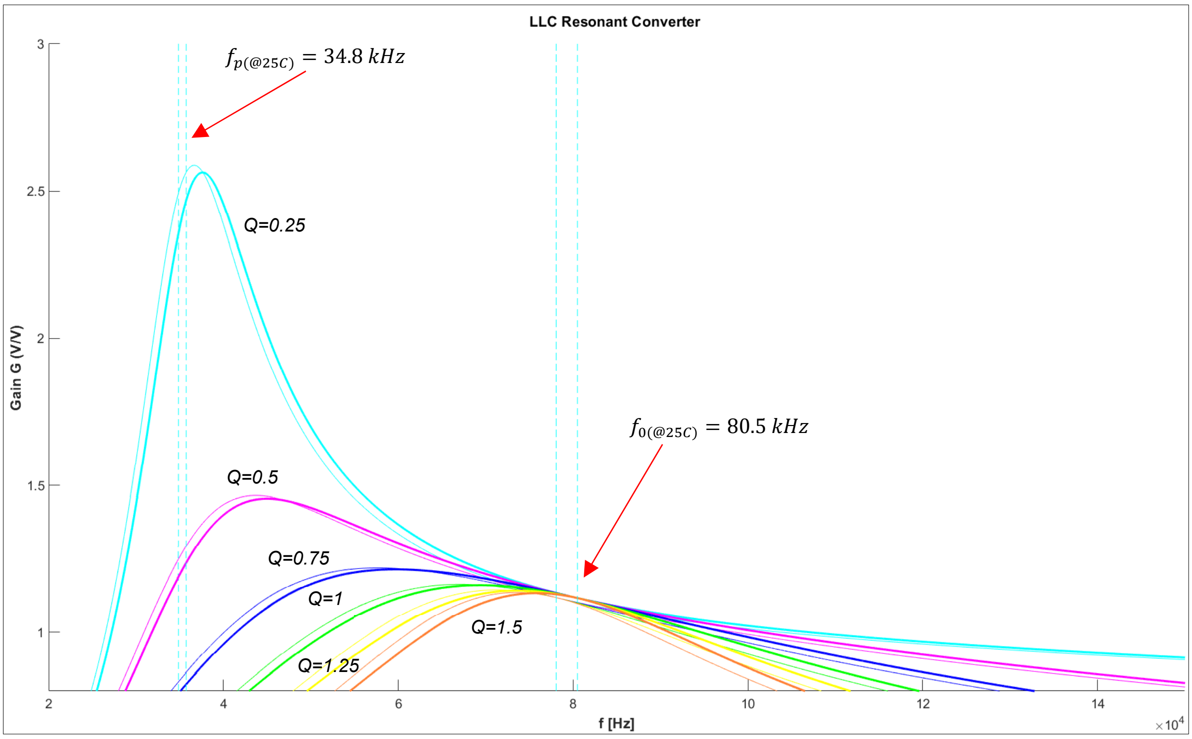

Fig. 12. *Gain characteristics of investigated LLC resonant converter at steady state (thick) and switch-on (thin).*

Upon examining Figure 12 one can infer that the resonant frequency as well as individual gain characteristics for selected values of *Q* factor were noticeably shifted towards higher frequencies. The change in resonant frequencies for primary inductance L_P and resonant capacitor C_{r4}, and for leakage/resonant inductance L_r and resonant capacitor C_{r4}, were about 1 kHz and 2.5 kHz, respectively. The observed shift in f_0 will have a measurable impact on how the current flowing through the LLC resonant tank will be shaped. If the LLC converter were finely tuned to operate at resonant frequency $f_{0(@25)}$, its operating point at higher temperature would be out of resonance, and therefore the current would somewhat deviate from the preferable almost purely sinusoidal shape.

In order to evaluate the impact of temperature on the resonant tank components in the investigated LLC SMPS, the converter was kept running at full output power P_{OUT} until the moment of reaching the thermal steady state of the entire system. At this point the temperature of each of the resonant circuit components was determined with the use of IR thermography. Thermographic cameras lend themselves readily to this purpose as temperature over larger areas has to be ascertained, and, due to high working voltages, contact measurements methods are considered inappropriate from a safety point of view. The results of thermographic measurements in the form of the thermal images registered at the steady-state conditions are presented in Figure 13.

As shown, the maximum operating temperature for resonant capacitor C_{r4} (in the actual circuit, capacitor C_{r4} consists of a number of individual XR7 surface mount capacitors arranged in a configuration satisfying the AC-current requirement resulting from the level of electric power being converted) was about 105 ˚C, which coincidently matches the maximum internal ambient in the test chamber at which the parameters of the LLC resonant tank were determined. The constructed integrated LLC transformer and the core it was wound upon, similarly to the capacitor, were running at a temperature nearing 105 ˚C. As a consequence, it was expected to observe a comparable shift in the resonant frequency of the LLC converter, examined as a whole, to that calculated for the individual resonant circuit components. According to the calculations and the gain characteristics in Figure 11, resonant frequency $f_{0(@25)}$, determined at the moment of the switch-on, should be about 78 kHz. The verification of the converter's exact switching frequency was not entirely straightforward, as the measurement was impacted by minor ripples in input voltage V_{DC}, which is the voltage across a so-called bulk capacitor. The bulk capacitor in the vast majority of AC/DC converters is supplied directly from some sort of a bridge rectifier, and the voltage across it undergoes certain fluctuations due to charging and discharging cycles of the capacitor dictated by the frequency of AC supply voltage and output power drawn. Nevertheless, the operating frequency can be ascertained with a satisfying precision from the shape of the resonant tank current waveform shown in Figure 14 captured at the switch-on of the converter. The converter's operating/switching frequency f_s was determined to be about 71.74 kHz as the period of an individual cycle was measured to be about 13.94 µs. The actual resonant frequency was estimated to be about 78.7 kHz (12.701 µs).

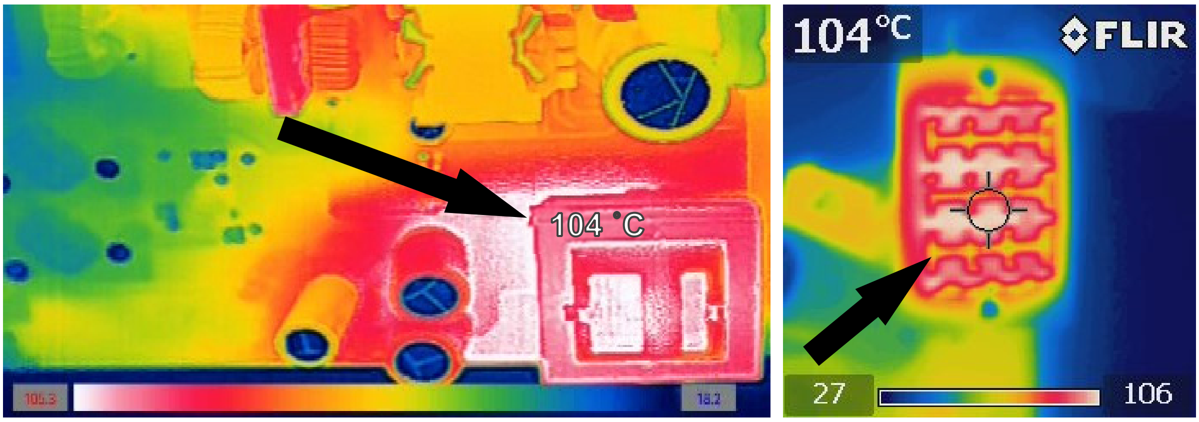

Fig. 13. *Thermal image of investigated LLC transformer (left) and resonant capacitor C_{r4} (right) at thermal steady state.*

From the very same figure one can conclude that resonant frequency $f_{0(@25)}$ is somewhat higher than switching frequency f_s, as the resonant current waveform has distinctive distortions in its shape in the form of visible steps. This is in compliance with the converter operating at $f_s < f_0$. Resonant frequency f_0 in an actual LLC SMPS is usually also affected by secondary side circuitry, and its contribution to secondary-side leakage inductance that translates via a turn ratio squared to the primary side, and increases primary-side leakage inductance and thus impacts a resonant frequency of a given LLC converter. The primary-side leakage inductance can be also increased by incorporating a small inductor in series with the integrated transformer and thus adding to the primary leakage inductance L_{lkp} shown in Figure 4, with the result that the resonant frequency can be finely tuned to the switching frequency. The other manoeuvre that would eventually lead to the two frequencies being identical would be redesigning of the transformer windings, thus modifying the component's turn ratio and the gain G (see Figure 5). This would steer the switching frequency f_s toward higher frequencies. It has to be noted that by doing so the leakage inductance of the integrated LLC transformer would be altered, hence the resonant frequency f_0 for the resonant capacitor C_r and the resonant inductance L_r is bound to somewhat differ from that registered for the LLC magnetic component consisting of the original number of turns.

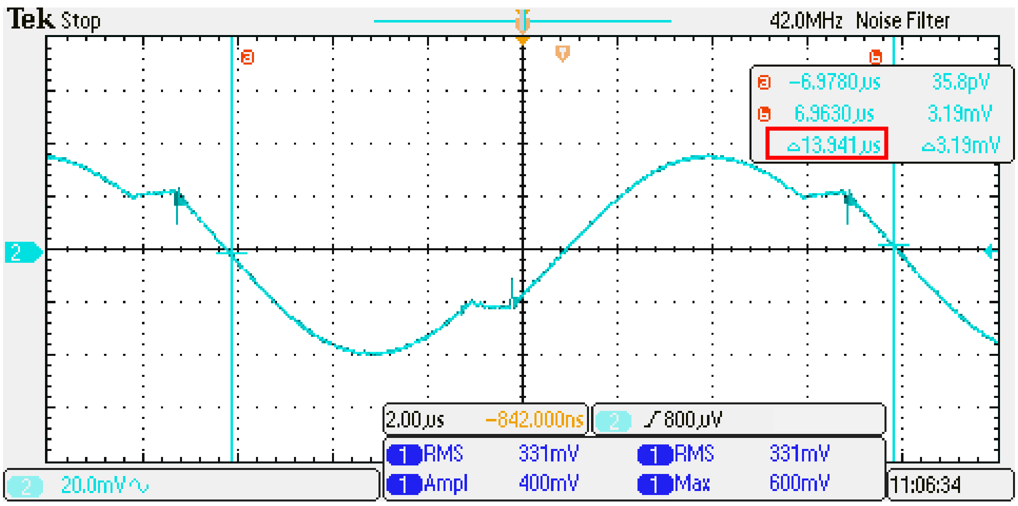

Fig. 14. *Resonant tank current waveform registered at switch-on (25 ˚C) for P_{OUT} = 180 W.*

At the moment of reaching the thermal steady state of the system the thermographs of Figure 13 were captured and the shape of the resonant tank current waveform was recorded once again (see Figure 15). As can be inferred, the shape of the current flowing through the resonant circuit has been slightly altered leading to a somewhat lower dissonance between f_s and f_0, and the observed distortions are fractionally less marked. This is due to the resonant frequency f_0 being higher for the thermal steady state than at the moment of the switch-on. It has to be concluded that the observable alternations in the way the current is shaped by the resonant circuit are minor and, as such, should not have any impact, or only negligible impact, on the operation of the LLC resonant converter as a whole. Resonant frequency $f_{0(@105}$ was estimated from Figure 15 to be about 81.29 kHz (12.301 µs) which is in compliance with the calculated shift in the resonant frequency of about 2.5 kHz.

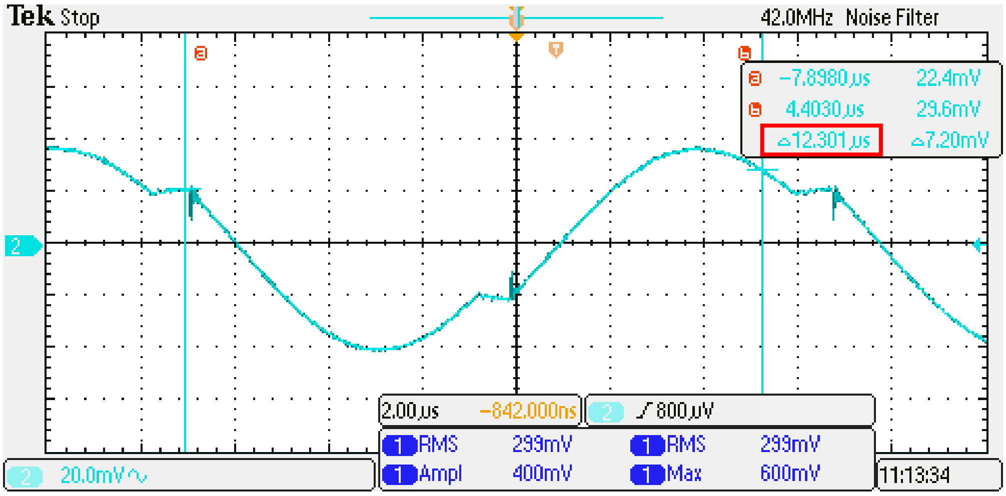

Fig. 15. *Resonant tank current waveform registered at thermal steady state for POUT = 180 W.*

4. Conclusions

This paper examines the evolution of parameters of an LLC resonant tank with temperature and thus the impact of operating temperature on the resonant frequency, current waveforms through the resonant circuit and the operation of the converter as a whole. A wide range of resonant capacitors of different construction and dielectric mediums was investigated along with the primary and leakage inductance of the constructed integrated LLC transformer. It was found that capacitors of particular dielectric materials, namely X8G and C0G/NP0, display superior thermal stability, hence making them preferable candidates to employ in resonant tanks from a thermal performance point of view. Double and single metallized PP film capacitors were shown to be of relatively high quality, as their capacitance displayed only a minor decrease with rising temperature. The primary inductance of the tested LLC integrated transformer showed deviations with temperature typical for the 3C95 ferrite material the transformer's core was made of. Generally, the evolution of primary inductance with temperature will depend on the magnetic material utilized in the design of the LLC transformer and the thermal stability of the material's magnetic permeability. As anticipated, the leakage inductance of the transformer remained largely unaffected by temperature swings. The observed shift in the resonant frequency of the LLC converter due to the higher operating temperature of resonant tank components at the thermal steady state was comparable to the estimate based on the measurements in the thermal test chamber. Somewhat less profound distortions in the resonant current waveforms for the highest operating temperatures should not bear an evident impact on the efficiency of power conversion and the general performance of the examined LLC converter.

REFERENCES

[1] R. W. Erickson, D. Maksimovic, "Fundamentals of Power Electronics", Second edition, Kluwer Academic Publishers, 2001,ISBN 0-7923-7270-0, pp. 728 – 782.

[2] Chin-Yuan Hsu, Jian-Ting Lai, Ming-Che Lin, Ming-Kai Yang, Ming-Jyun Li, Ren-Wei Huang, "The design and implementation of LLC resonant half-bridge converter with natural interleaved power-factor-correction", in *IEEE Ninth Intern. Conf. on Power Electronics and Drive Systems*, Singapore, Dec 2011.

[3] S. A. Ansari, J. Davidson, M. Foster, "Inserted-shunt Integrated Planar Transformer with Low Secondary Leakage Inductance for LLC Resonant Converters", IEEE Transactions on Industrial Electronics (Early Access), Apr 2022.

[4] Bo Yang, F.C. Lee, A.J. Zhang, Guisong Huang, "LLC Resonant Converter for Front End DC/DC Conversion", in *17th Annual IEEE Applied Power Electronics Conference and Exposition*, Dallas, TX, USA, March 2002.

[5] Binqi Li, Xiangjun Zhang, Dibin Zhou, Shixin Sun, Yijie Wang, Dianguo Xu, "Soft-switching Characteristics Analysis Based on LLC Resonant Converter", in *2018 IEEE Transportation Electrification Conference and Expo, Asia-Pacific (ITEC Asia-Pacific)*, Bangkok, Thailand, June 2018.

[6] Ferroxcube Data Handbook, Soft Ferrites and Accessories, Ferroxcube, 2013, p.94.